

## A comparison of ambipolar diffusion coefficients in meteor trains using VHF radar and UV lidar

Phillip B. Chilson, Peter Czechowsky, and Gerhard Schmidt

Max-Planck-Institut für Aeronomie, Katlenburg-Lindau, Germany

### Abstract.

In this paper we present the first comparative estimations of ionic diffusion rates for sporadic meteor trains near the mesopause made using VHF radar and UV Rayleigh lidar observations. In both cases we initially assumed that the meteor trains dissipate primarily through ambipolar diffusion. For the radar data, the diffusion coefficient within the meteor train was determined from the decay rate of the backscattered power. From the the lidar data we then calculated profiles of the atmospheric temperature and density in the height range at which the meteor echoes were detected. These data were used to estimate the ambipolar diffusion coefficients that would result assuming different species of ions. Our results appear consistent with the notion that short-lived underdense meteor trains in the height range of 85 – 95 km decay primarily by ambipolar diffusion. However, the diffusion coefficients obtained from the radar observations were smaller than those found from the lidar data assuming metal meteoric ions. One possible explanation could be that the radar meteor echoes resulted from ionized constituents of the atmosphere.

### Introduction

When a meteor ablates in the Earth's atmosphere, it produces a cylindrical column of ionization that can be detected by VHF radars as a meteor train echo. After its formation, the ionization begins to dissipate by, among other processes, ambipolar diffusion, eddy diffusion, and recombination. The result is a decrease in the echo power received by the radar. Which decay mechanism dominates depends on the type of meteor (e.g., underdense or overdense) and its height of ablation. It is generally assumed that for underdense trains occurring near the mesopause and lasting less than a few seconds, ambipolar diffusion primarily determines the rate of decay [e.g., Jones, 1975; Thomas *et al.*, 1988].

Consider those meteor trains assumed to decay primarily through ambipolar diffusion. Using laboratory measurements of ionic mobilities and model atmospheric data, one can calculate the ambipolar diffusion coefficient  $D_a$  of the trains. The calculated values of  $D_a$  can then be compared with those obtained directly from

radar data. A departure between the radar- and lidar-derived diffusion coefficients indicates regions of the atmosphere where decay processes other than ambipolar diffusion are active.

We present the first observations of sporadic meteors made with a VHF radar while simultaneously monitoring the temperature and density of the atmosphere using a UV Rayleigh lidar. Assuming the meteor train to consist of a single type of ion having a known mobility, we used the lidar-derived profiles of temperature and density to calculate  $D_a$  as a function of height. These values were then compared with the diffusion coefficients measured with the radar.

### Experiment

The SOUSY VHF radar was operated on July 31 – August 1, 1995 in a mode suitable for the detection of meteor trains. The radar transmits at 53.5 MHz with a peak power of 600 kW. Data were collected for approximately 25 h (12:22 – 13:37 LT) while cycling between six different beam orientations: one vertical, four having a 12° zenith angle, and one configuration consisting of four split beams having approximately the same reduced gain and a 30° zenith angle. Due to electrical and spatial weighting of the single Yagis, the two-way side lobes are suppressed by 43 dB. When oriented vertically, the one-way half-power half-width of the main beam was 2.5°. The range resolution was 600 m. The received radar signal for each beam was stored as a 295-pt complex time series having an effective sampling interval in the time series of 22.67 ms. For a more thorough discussion of the radar see Schmidt *et al.* [1979].

The SOUSY UV Rayleigh lidar is located 26 km from the radar site and uses a XeF excimer laser (351 nm) with a maximum pulse energy of about 200 mJ. A brief technical description of the lidar system has been given in Czechowsky *et al.* [1991]. The lidar was operated with a height resolution of 600 m and a time resolution of 40 s. Data were collected over a 5 h period (23:00 – 04:00 LT). The upper range of the observations depends on the sky conditions and the amount of integration time. Typically the temperature profiles to be discussed in this work extend up to 90 – 95 km.

### Analysis

We begin our analysis by considering how diffusion affects the decay rate of meteor echoes. Assuming am-

bipolar diffusion to be the dominant decay mechanism, *Kaiser* [1953] has shown that the backscattered power from an underdense meteor echo can be written as

$$P(t) = P(0) \exp \left[ -\frac{32\pi^2 D_a}{\lambda^2} t \right], \quad (1)$$

where  $P(0)$  is the initial echo power,  $\lambda$  is the radar wavelength,  $t$  is the elapsed time, and  $D_a$  is the ambipolar diffusion coefficient. From (1) together with our observations of underdense meteor trains, we can obtain values of  $D_a$  as a function of height. We refer to ambipolar diffusion coefficients obtained from radar data using (1) as  $D_R$ .

Next we examine how the properties of the neutral atmosphere and the charged ions affect  $D_a$ . To begin we consider a dilute system of ions and electrons in a neutral gas. For the case of a vanishing electric field, the ionic diffusion coefficient  $D_i$  ( $\text{m}^2 \text{s}^{-1}$ ) is given through the Einstein relation as

$$D_i = \frac{kT}{e} \left( \frac{T}{273.16 \text{ K}} \right) \left( \frac{1.013 \times 10^5 \text{ Pa}}{p} \right) K_o, \quad (2)$$

where  $k$  is the Boltzmann constant,  $e$  is the ionic charge, and  $T$  and  $p$  are the temperature and pressure of the neutral gas, respectively [McDaniel and Mason, 1973].  $K_o$  is the zero-field reduced mobility of the ions and has the units of  $\text{m}^2 \text{V}^{-1} \text{s}^{-1}$ . Note that in (2)  $D \propto T/\rho$ , which is the correct dependence if long-range forces between ions and molecules are assumed [see, Jones, 1995]. From (2) we finally obtain the coefficient of ambipolar diffusion through the relation

$$D_a = D_i \left( 1 + \frac{T_e}{T_i} \right), \quad (3)$$

where  $T_e$  and  $T_i$  are the electron and ion temperatures, respectively. Assuming a meteor train consists primarily of a single type of ion, then (2) and (3) can be used in (1) to predict the decay rates of meteor train echoes.

## Lidar Data

Height profiles of the atmospheric temperature and density can be calculated from lidar data for altitudes at which transmitted ultraviolet light pulses backscatter primarily from air molecules [Chanin and Hauchecorne, 1980]. We have done this using a method similar to that of Shibata *et al.* [1986]. The resulting height profiles of the temperature for the evening of July 31 to August 1 are shown in Figure 1. The profiles correspond to five consecutive 60-min time averages of the lidar data, and they have been offset in temperature by 100 K.

Having the atmospheric temperature and pressure we can use (2) and (3) to calculate  $D_a$ , given  $K_o$ ,  $T_e$ , and  $T_i$ . It is common to assume that the ions and electrons rapidly reach thermal equilibrium with the neutral gas through collisional processes. Jones [1975] support the assumption for heights up to 100 km. For such a case  $D_a = 2D_i$ , and the only undetermined quantity is  $K_o$ .

Jones and Jones [1990] have used values of  $K_o$  for meteoric ions in their analysis of train diffusion. As they show, the value of  $K_o$  for metal ions depends almost exclusively on the mass number, and they choose  $\text{Mg}^+$  and  $\text{Fe}^+$  as having mass numbers that bracket those of the dominant species of meteoric ions. We begin by considering the mass number of 40, which lies between those for  $\text{Mg}^+$  (24) and  $\text{Fe}^+$  (56). We will denote this ion as  $\text{M}^+$ . Using the mobility equation given in Jones and Jones [1990] we found  $K_o = 2.5 \times 10^{-4} \text{ m}^2 \text{V}^{-1} \text{s}^{-1}$  for  $\text{M}^+$  in  $\text{N}_2$ .

We may now proceed to calculate the lidar-derived values of the ambipolar diffusion coefficient, which will be denoted by  $D_L$ . Five separate height profiles of  $D_L$  have been generated using the data shown in Figure 1 along with the corresponding density measurements. These are shown in Figure 2. Additionally, values of diffusion coefficients corresponding to the temperature and pressure data from the CIRA-1986 reference atmosphere [Fleming *et al.*, 1990] have been calculated,

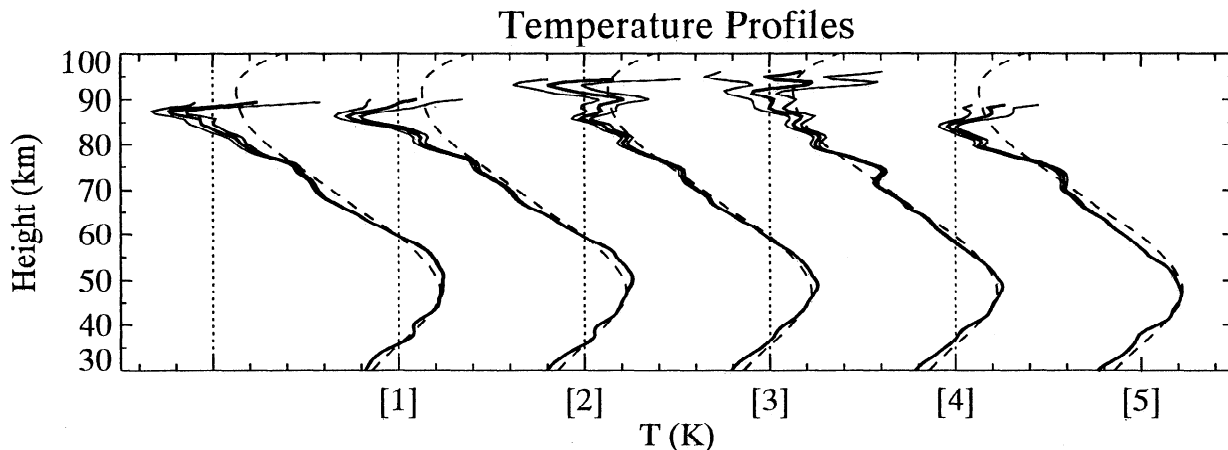


**Figure 1.** Temperature profiles (heavy solid lines) together with their standard deviations (light solid lines) derived from lidar observations. The vertical dotted lines indicate a 150-K reference temperature. The dashed curves show temperature profiles taken from the CIRA-1986 reference atmosphere. Each tick on the abscissa corresponds to 10 K.

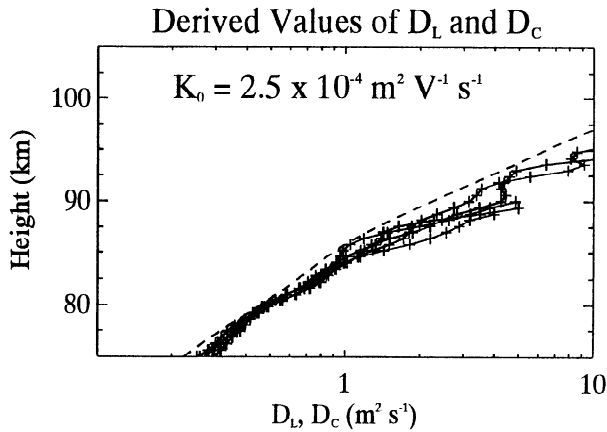


**Figure 2.** Calculated profiles of the ambipolar diffusion coefficient based on lidar observations  $D_L$  (connected plusses) and the CIRA-1986 reference atmosphere  $D_C$  (dashed curve).

where the values for 50° N during July have been used.

Figure 2 reveals two interesting features of the height profiles of  $D_L$  and  $D_C$ . Firstly, above 85 km the profiles of  $D_L$  show a wide spread in values. The differences in  $D_L$  are at some heights 1 - 2  $\text{m}^2 \text{s}^{-1}$ . Although some of the variation can be attributed to estimation uncertainties, the temperature profiles in Figure 1 also show significant structure at these altitudes. Consequently, estimates of the ambipolar diffusion coefficient obtained from radar observations taken over the same time and height interval should have similar variations. Secondly, the estimates of the diffusion coefficient based on the reference atmosphere data  $D_C$  are consistently smaller than those based on the lidar observations  $D_L$ . This will be shown to be important when interpreting the nature of the ionic diffusion.

**Radar Data**

The radar data were processed off line using a series of filters and test criteria. First, for a data record to be considered for further analysis, the signal-to-noise ratio (SNR) was required to exceed a 2-dB level over at least 6 contiguous time-series points (0.14 s). This places an upper limit on the value of  $D_R$  that can be estimated. Meteor trains that form at high altitudes (large  $D_a$  values) can only exceed the 2-dB level for 0.14 s if the initial SNR value is large. For an initial SNR of 40 dB the maximum value of  $D_R$  that can be calculated is 6.3  $\text{m}^2 \text{s}^{-1}$ , and for an SNR of 50 dB the maximum value of  $D_R$  is 7.9  $\text{m}^2 \text{s}^{-1}$ . For our data, 95% of the initial SNR values were less than 43 dB, and 99% were less than 50 dB. The decay rate of the echo signal was then found by fitting a straight line to the logarithm of the radar SNR. If the fit was good, then the echo was attributed to an underdense meteor, and the diffusion coefficient was found using (1). Figure 3 shows an example of the SNR plotted as a function of time for an underdense meteor.

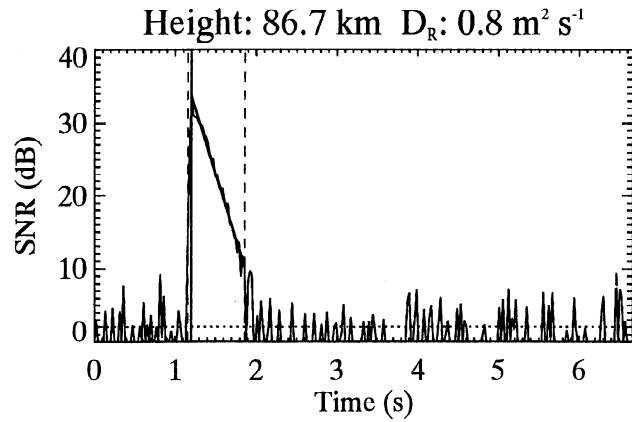


**Figure 3.** The time series of power showing how  $D_R$  is calculated from the time rate of decay. The dotted horizontal line shows the 2-dB threshold, the dashed vertical lines indicate the range in which the SNR exceeds the 2-dB threshold, and the solid vertical line marks the time of the peak SNR.

We have obtained values of  $D_R$  using the vertical beam and the four off-vertical beams having zenith angles of 12°. The width of the vertical and off-vertical beams were the same to within 5%. The beam orientation consisting of the four split beams was not used since the different lobes had slightly different zenith angles, which made it difficult to locate a given meteor echo in height. A scatter plot of  $D_R$  versus height is presented in Figure 4. There are two clusters of data centered at heights of roughly 88 and 100 km. We should mention that when the radar beam is oriented 12° off vertical, a grating lobe (not to be confused with side lobes) appears at a zenith angle of 32° that is 18 dB (two-way power) below the main beam [see for example, Czechowsky et al., 1988]. The grating lobe results

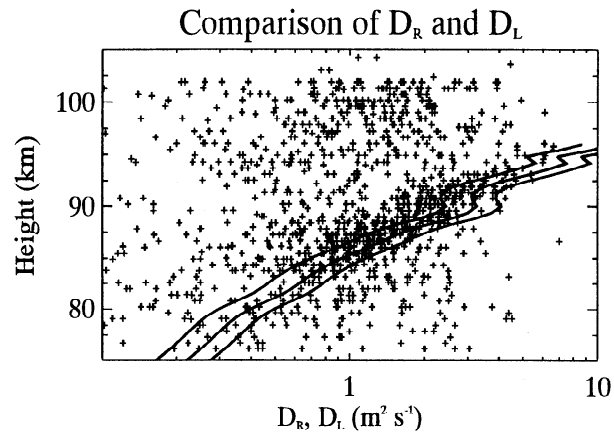


**Figure 4.** Scatter plot of the diffusion coefficients obtained from the radar data  $D_R$  plotted as a function of height. Also shown are three profiles calculated from the lidar data  $D_L$  for assumed values of  $K_0$  equal to  $1.5 \times 10^{-4} \text{m}^2 \text{V}^{-1} \text{s}^{-1}$  (leftmost curve),  $2.0 \times 10^{-4} \text{m}^2 \text{V}^{-1} \text{s}^{-1}$  (middle curve), and  $2.5 \times 10^{-4} \text{m}^2 \text{V}^{-1} \text{s}^{-1}$  (rightmost curve).

from the way in which the Yagi antenna elements are fed. Since meteor echoes can be quite large, trains are also detected in the grating lobes. The upper cluster of data are almost certainly due to grating-lobe echoes. A meteor detected at a height of 88 km with the 32°-grating lobe would appear in the scatter plot at 101 km.

Also shown in Figure 4 are three profiles of  $D_L$  calculated for different assumed values of  $K_o$ . Each profile represents a time average over the 5-h lidar observational period. The assumed values of  $K_o$  extend from  $1.5 \times 10^{-4}$  to  $2.5 \times 10^{-4} \text{ m}^2 \text{ V}^{-1} \text{ s}^{-1}$ . Based on Jones and Jones [1990], the bracketing values of  $K_o$  for metallic meteor ions lie between  $2.4 \times 10^{-4}$  and  $2.9 \times 10^{-4} \text{ m}^2 \text{ V}^{-1} \text{ s}^{-1}$ . This range of  $K_o$ , however, yields values of  $D_L$  larger than estimated by the radar. In fact, agreement between the radar and lidar data appears best for  $K_o = 1.5 \times 10^{-4}$  and  $2.0 \times 10^{-4} \text{ m}^2 \text{ V}^{-1} \text{ s}^{-1}$ . Recall that the profile of  $D_C$  shown in Figure 2 is consistently larger than those for  $D_L$ . A comparison of  $D_R$  and  $D_C$  (without the  $D_L$  values) leads to the false interpretation that agreement is best obtained using  $K_o = 2.5 \times 10^{-4} \text{ m}^2 \text{ V}^{-1} \text{ s}^{-1}$ .

## Discussion

Many factors determine the decay rate of the ionization produced by meteor ablation. We have based our analysis on the assumption that the short-lived underdense meteor trains that we observed decayed primarily by ambipolar diffusion. At what altitudes should we expect this assumption to be valid. Using theory and empirical data, Jones [1975] found the height range to extend between approximately 85 and 95 km. Below 85 km the oxidation-dissociation process plays a significant role, whereas above 95 km, secondary reflection points resulting from wind-induced distortions of the plasma column decrease the values of  $D_R$ . If processes other than ambipolar diffusion were active, then the time rate of decay of the meteor column would be enhanced, leading to larger apparent diffusion coefficients. The values of  $D_R$  were actually less than those of  $D_L$  assuming metal meteoric ions. Furthermore, the profiles of  $D_L$  show good agreement with main distribution of  $D_R$  in the height range of 85–95 km, if we assume  $K_o = 1.5 \times 10^{-4}$ – $2.0 \times 10^{-4} \text{ m}^2 \text{ V}^{-1} \text{ s}^{-1}$ . Although these values of  $K_o$  are smaller than those expected for meteoric metal ions, the observations appear consistent with the notion that meteor trains we have considered decayed primarily by ambipolar diffusion.

Why should the values of  $D_R$  and  $D_L$  show better agreement for such small values of  $K_o$ ? One possible explanation is that the radar meteor echoes resulted not from meteor particles but from constituents of the atmosphere that ionized during meteor ablation. Spectral analysis studies have shown meteor trains to con-

tain such ions as  $\text{O}_2^+$ ,  $\text{N}_2^+$ , and  $\text{NO}^+$  [Bronshten, 1983]. For example, the zero-field reduced mobilities for  $\text{N}_2^+$  in  $\text{N}_2$  and  $\text{O}_2^+$  in  $\text{O}_2$  are reported to be  $2.24 \times 10^{-4}$  and  $1.87 \times 10^{-4} \text{ m}^2 \text{ V}^{-1} \text{ s}^{-1}$ , respectively [McDaniel and Mason, 1973], which might account for the observations. However, further study is required before any firm conclusions can be drawn along these lines.

**Acknowledgments.** We are grateful to both William Jones and Jürgen Klostermeyer for their helpful comments while preparing this paper. We also appreciate the comments from two anonymous referees.

## References

- Bronshten, V. A., *Physics of Meteoric Phenomena*, D. Reidel Publishing Company, Dordrecht, 1983.
- Chanin, M. L., and A. Hauchecorne, Density and temperature profiles obtained by lidar between 35 and 70 km, *Geophys. Res. Lett.*, **7**, 565–568, 1980.
- Czechowsky, P., I. M. Reid, and R. Rüster, VHF radar measurements of the aspect sensitivity for the summer polar mesopause over Andenes (69°N, 16°E) Norway, *Geophys. Res. Lett.*, **15**, 1259–1262, 1988.
- Czechowsky, P., B. Inhester, J. Klostermeyer, and G. Schmidt, Simultaneous radar and lidar observations during the DYANA-campaign, in *Proceedings 10th ESA Symposium on European Rocket and Balloon Programmes and Related Research*, pp. 399–405, 1991.
- Fleming, E. J., S. Chandra, J. J. Barnett, and M. Corney, Zonal mean temperature, pressure, zonal wind and geopotential height as a function of latitude, *Adv. Space Res.*, **10**(12), 11–59, 1990.
- Jones, J., On the decay of underdense radio meteor echoes, *Mon. Not. Roy. Astr. Soc.*, **173**, 637–647, 1975.
- Jones, W., The decay of radar echoes from meteors with a particular reference to their use in the determination of temperature fluctuations near the mesopause, *Ann. Geophys.*, **13**, 1104–1106, 1995.
- Jones, W., and J. Jones, Ionic diffusion in meteor trails, *J. Atmos. Terr. Phys.*, **52**, 185–191, 1990.
- Kaiser, T. R., Radio echo studies of meteor ionization, *Phil. Mag.*, **2**, 495–544, 1953.
- McDaniel, E. W., and E. A. Mason, *The Mobility and Diffusion of Ions in Gases*, John Wiley and Sons, New York, 1973.
- Schmidt, G., R. Rüster, and P. Czechowsky, Complimentary code and digital filtering for detection of weak VHF radar signals from the mesosphere, *IEEE Trans. Geosci. Electron.*, **GE-17**, 154–161, 1979.
- Shibata, T., M. Kobuchi, and M. Maeda, Measurements of density and temperature profiles in the middle atmosphere with a XeF lidar, *Appl. Opt.*, **25**, 685–688, 1986.
- Thomas, R. M., P. S. Whitham, and W. G. Elford, Response of high frequency radar to meteor backscatter, *J. Atmos. Terr. Phys.*, **50**, 703–724, 1988.

Phillip B. Chilson, Peter Czechowsky, and Gerhard Schmidt, Max-Planck-Institut für Aeronomie, Postfach 20, D-37189 Katlenburg-Lindau, Germany.

(received April 2, 1996; revised July 4, 1996; accepted July 25, 1996.)